IEEE Access
Multidisciplinary | Rapid Review | Open Access Journal

Received 1 July 2022, accepted 17 August 2022, date of publication 24 August 2022, date of current version 31 August 2022.

Digital Object Identifier 10.1109/ACCESS.2022.3201205

RESEARCH ARTICLE

A Single-Feed Wideband Circularly Polarized Dielectric Resonator Antenna Using Hybrid Technique With a Thin Metasurface

ARSLAN KIYANI[1], (Member, IEEE), NASIMUDDIN NASIMUDDIN[2], (Senior Member, IEEE), RAHEEL M. HASHMI[1], (Senior Member, IEEE), AFFAN AZIZ BABA[1], (Member, IEEE), SYED MUZAHIR ABBAS[1,3], (Senior Member, IEEE), KARU P. ESSELLE[4], (Fellow, IEEE), AND ABDELHADY MAHMOUD[5], (Member, IEEE)

[1]School of Engineering, Faculty of Science and Engineering, Macquarie University, Sydney, NSW 2109, Australia
[2]Institute for Infocomm Research, Agency for science, Technology and Research (A*STAR), Singapore 138632
[3]BENELEC, Botany, Sydney, NSW 2019, Australia
[4]School of Electrical and Data Engineering, University of Technology Sydney (UTS), Sydney, NSW 2007, Australia
[5]Faculty of Engineering, Benha University, Benha 13512, Egypt

Corresponding author: Arslan Kiyani (arslan.kiyani@mq.edu.au)

This work was supported in part by the Australian Research Council, Macquarie University Research Excellence Scholarship (MQRES) Scheme; and in part by Macquarie University COVID Recovery Fellowship.

ABSTRACT A compact metasurface-based circularly polarized (CP) dielectric resonator antenna (DRA) is proposed with wideband characteristics. The antenna forms a very simple structure, composed of a rectangular DR, a single coaxial probe, and plus-shaped unit cells-based metasurface. The metasurface is realized on a grounded FR-4 substrate. Next, a rectangular DR is loaded centrally over the metasurface. The DR is fed with a perturbed probe feed at an appropriate angle of (θ=29°), along the diagonal line. Thus, a novel hybrid technique involving the angle of feed location from the center of DR, and the $N \times N$ unit cells-based metasurface is utilized for generating a wideband CP radiation. The resonance from the rectangular DR and surface waves along the 7×7 plus-shaped unit cells-based metasurface is exploited to achieve a wide 3-dB axial ratio (AR) and impedance matching bandwidth. The fabricated antenna prototype used for the validation of predicted results confirms the successful implementation of the proposed technique. Measured results demonstrate a wide impedance bandwidth of 32% (3.6 GHz - 7.0 GHz) and an overlapping 3-dB AR bandwidth of 20.4% (4.2 GHz - 5.2 GHz). Moreover, the antenna adopts a left-hand circular polarization (LHCP) with 6-7 dBic measured gain within the operational frequency range. Overall, the proposed antenna offers low-profile, simplicity, ease of design, and high performance.

INDEX TERMS Circular polarization, CP feed, metasurface antenna, metamaterial, rectangular dielectric resonator, DRA, probe feed, coaxial, wideband.

I. INTRODUCTION

With the rapid deployment of 5G at our doorstep, forthcoming wireless solutions incorporate smart technologies and pose stringent expectations. The demand for compact, efficient, lightweight, wideband, and high-gain antennas is on the rise. Besides, polarization is considered one of the most significant performance features for antenna integration with modern communication systems [1]. Compared to linearly polarized antennas, circularly polarized (CP) antennas are gaining more recognition, owing to their salient advantages of low-cross talk, improved multipath rejections, and better mobility [2]. These features are extremely useful and have great significance in implementing various telecommunication systems and satellite applications. This includes radio frequency identification (RFID), radar technology, global

The associate editor coordinating the review of this manuscript and approving it for publication was Derek Abbott.

positioning systems, healthcare, and weather forecast. Furthermore, with ever-growing requirements of higher data rates and insensitivity to the transmitter and receiver orientation, low-profile wideband CP antennas are desired [3], [4]. Microstrip patch antennas offer polarization flexibility, planar structure, and ease of fabrication. They have long remained a suitable candidate for various wireless applications. Despite many advantages, patch antennas are constrained by their narrow bandwidth and low gain performance [5], [6]. Dielectric resonator antenna (DRA), on the other hand, offers an edge over microstrip antenna in multiple ways, such as small size, easily fed, metallic lossless, high-quality factor, higher radiation efficiency, and no surface wave excitation [7], [8].

The realization of circular polarization typically requires the generation of dual orthogonal modes with a 90° phase shift. In CP DRAs, this 90° phase shift is generated by making use of either single-point or multi-point feeding techniques [9], [10], [11], [12]. Dual and quadrature feeds are demonstrated to achieve wide impedance matching and 3-dB axial ratio (AR) bandwidth [11], [13], [14]. However, the implementation of these feeds requires power dividers or external hybrid couplers, which come with in [29]-creased complexity, and bigger antenna size. On the other hand, the requirement of CP radiation is particularly challenging to achieve over a wide range of frequencies, for designing a single-feed wideband CP DRA. Considering this, an increased amount of interest resulted in the design of various single-feed CP DRAs. These DRAs are demonstrated to enhance the CP radiation bandwidth such as CP radiation was generated by the perturbation method in [15], by a circular-sector-slot in a circular cylinder DR [16], square-slots in rectangular DR [17], hexagonal-shaped DR [18], and a slotted-square DR with parasitic strips [19] for omnidirectional radiation. In addition, various researchers have expanded the AR bandwidth of DRAs by using a high-order mode approach. For example, in the case of a cylindrical DRA [20], the fundamental mode HEM111 and high-order mode HEM113 were excited by designing two feed strips for achieving broadband CP radiation. While three orthogonal modes were excited simultaneously by employing a trapezoidal DRA in [21]. Numerous methodologies have also been reported to improve the performance of CP DRAs with array configurations. Some of these approaches include probe fed DRA array [22], rectangular DRA array [23], elliptical DRA array [24], and a 2 × 4 sequentially rotated DRA array [25]. One of the major drawbacks of these configurations is the requirement of a feeding network, which may lead to design complexities.

Recently, efforts have been dedicated to improving the performance parameters of antennas by employing metasurface structures [26]. Metasurface, owing to their property of manipulating the electromagnetic waves, are placed either above or beneath the patch/radiators for achieving wideband and high gain operation [27], [28], and more recently on the single layer. CP microstrip single feed antennas have been miniaturized with improved bandwidth by using metasurface structures. These include a reactive impedance surface (RIS) [29], [30], an artificial ground plane/metamaterial-surface based single dipole antenna [31], a metasurface based slotted-rectangular microstrip antenna [32], and a stacked asymmetric metasurface above the rectangular patch [33] for wide 3-dB AR bandwidth, and high gain, respectively. More recently, a wide selection of antennas combining patches and metasurface of various shapes and sizes are investigated [34], [35], [36], [37], [38], [39], [40], [41], [42], [43]. However, to the best of the author's research, literature review, and knowledge, no rectangular DR antenna is yet reported over a metasurface for achieving wideband CP characteristics.

In this paper, a metasurface-based rectangular DR is demonstrated by utilizing a single coaxial feed at a particular angle for wideband CP radiation. The rectangular DR is placed over a metasurface consisting of 7 × 7 unit cells etched on a grounded substrate and a coaxial feed. The DR is excited along the diagonal at a particular angle using a modified upper probe of coaxial feed to investigate a wide 3-dB AR bandwidth. The proposed hybrid technique combining the feed angle and well-matched metasurface demonstrates a wide 3-dB AR bandwidth within the 2-VSWR-frequency range. Also, a wider 20.4% 3-dB AR bandwidth with 6-8 dBic gain and 1-1.5 dB gain variation is demonstrated over the 3-dB AR bandwidth for the proposed

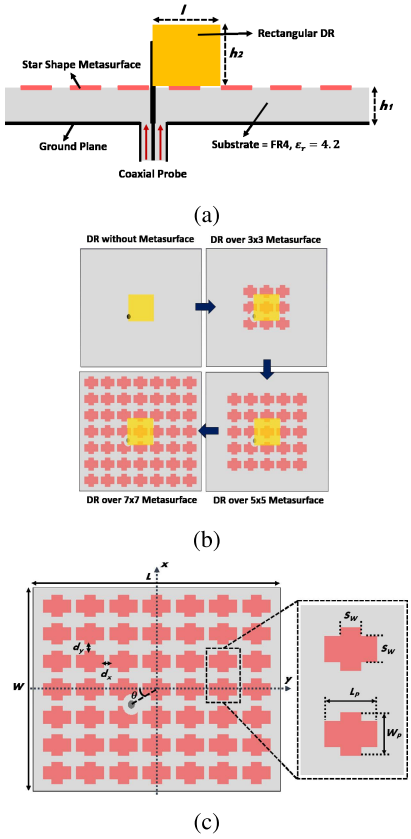

FIGURE 1. Schematics of wideband CP DRA over metasurface: (a) cross-sectional view (b) evolution towards final design (c) 7 × 7 array of plus-shaped unit cells-based metasurface.

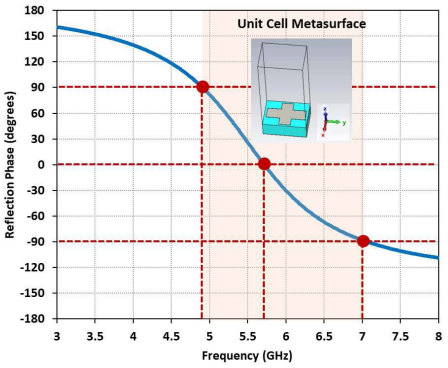

FIGURE 2. Reflection phase characteristic of unit-cell metasurface.

antenna. This antenna is designed and analyzed rigorously using CST microwave studio [44]. It can be utilized in defense and satellite communication applications such as weather radar systems or terrestrial microwave links etc.

II. ANTENNA STRUCTURE AND CONFIGURATIONS

This section presents a detailed design of the metasurface DR antenna based on the proposed hybrid technique. It also explains the antenna radiation mechanism by considering predicted results and E-Field characteristics. Later, a comparison of predicted and measured results is carried out for practical validation.

A. DESIGN PROCESS

Based on the analogy presented in [45], an exploded view of the proposed wideband CP DRA is depicted in Fig. 1 (a). The antenna design is comprised of rectangular DR, metasurface, a single substrate layer, and a ground plane. Initially, it follows the design procedure by having rectangular DR without any metasurface and later introducing periodic patches of $N \times N$ unit cell array metasurface, as illustrated in Fig. 1 (b). The rectangular DR is designed using TMM10i dielectric substrate ($h_2 = 6.5$ mm, $\epsilon_2 = 10.2$, $tan\delta = 0.002$) with the following dimensions (length, l = 14.9 mm and width, w = 12.6 mm) on the middle of a FR4 substrate. A $N \times N$ unit cell metasurface (where $N = 7$) is realized on a grounded FR4 dielectric substrate ($h_1 = 3.2$ mm, $\epsilon_1 = 4.2$, and $tan\delta = 0.022$), as shown in Fig. 1 (c). The overall size of this FR4 substrate is 55 mm × 76 mm. Whereas, the metasurface unit cell takes the shape of a plus with dimensions $S_w = 2.5$ mm, $W_p = 6.0$ mm, $L_p = 8.76$ mm, each separated by distance dx (in normal plane) and dy (in azimuth plane), respectively, for maintaining the periodicity. Generally, square, and rectangular-shaped metasurfaces have been utilized by various researchers previously with limitations of the narrow band. Therefore, a plus-shaped metasurface is considered here because of its potential wideband response. From the design perspective, a unit cell should have a reflection phase response of (±90°) exceeding the required operating frequency band [32]. To demonstrate this, the reflection phase characteristics of the proposed metasurface are investigated and shown in Fig. 2. The zero-degree reflection phase is located at 5.75 GHz with the reflection phase bandwidth (±90°) ranging from 4.9 GHz to 7 GHz, demonstrating the broadband response of the proposed metasurface. The metasurface unit cells are separated by 1.46 mm and 1.5 mm in both normal and azimuth plane. The antenna structure is then excited with a single coaxial feed positioned at $[x_o \times \cos(\theta), x_o \times \sin(\theta)]$, $[x_o = 7.5$ mm, $\theta = 29°]$ from the center of DR. The coaxial feed location is optimized along the diagonal line direction on the rectangular DR for a wideband CP radiation [32]. Lastly, the metallic part around the feed location from the metasurface is removed with a radius of 2.0 mm, to avoid any deterioration of the results due to the contact between the coaxial feed and unit cells.

B. OPERATING PRINCIPLE AND NUMERICAL STUDIES

A metasurface being the 2-D equivalent of 3-D metamaterial is considered a surface distribution of electrically small scatterers, which can be utilized to control and manipulate the electromagnetic waves and the radiation mechanism of primary radiators [28]. The extra resonance for the radiation structure can be yielded by combining the primary radiator with a finite-sized metasurface [46]. The surface waves which propagate on the metasurface structure produce these extra resonances. The surface wave resonances generated on a finite metasurface structure depends on the number of unit cells and periodicity among them, which can be qualitatively calculated by he cavity model and transmission line model, as presented in [28] as:

$$\beta_{SW} \times L_{MS} = \pi \tag{1}$$

where, β_{SW} denotes the propagation constant of the surface wave resonances, and L_{MS} is the metasurface structure length, as given by:

$$L_{MS} = N \times P \tag{2}$$

where, N is the number of metasurface unit-cells, and P is the periodicity among them. Replacing value of L_{MS} in (1), we get:

$$\beta_{SW} = \frac{\pi}{N \times P} \tag{3}$$

From [47], the propagation constant of the surface waves travelling and decaying away from the metasurface are related to the decay constant (α) and the frequency (ω), using the following equation:

$$\beta_{SW} = \sqrt{\eta^2\omega^2 + \alpha^2} \tag{4}$$

The propagation constant of the transverse magnetic (TM) and transverse electric (TE) can be computed by the following expressions:

$$\beta_{TM} = \frac{\omega}{c}\sqrt{1 - \frac{Z^2_{Metasurface}}{\eta^2}} \tag{5}$$

$$\beta_{TE} = \frac{\omega}{c}\sqrt{1 - \frac{\eta^2}{Z^2_{Metasurface}}} \tag{6}$$

where, ω is the angular frequency, c is the speed of light, η is the intrinsic impedance, and $Z_{Metasurface}$ represents the surface impedance of the metasurface structure.

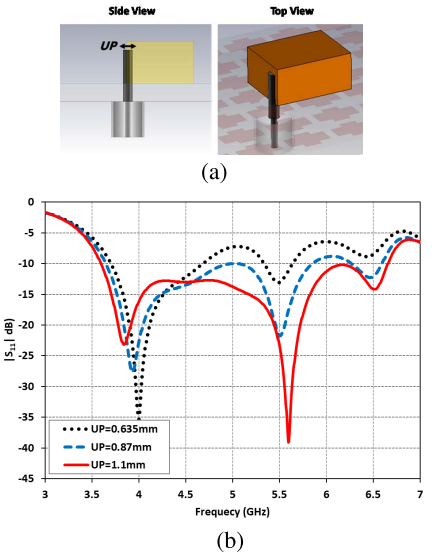

FIGURE 3. Varying upper probe UP of the coaxial feed to improve impedance matching bandwidth, so as to complement wideband 3-dB AR bandwidth (a) side and top view of UP (b) $|S_{11}|$ characteristics.

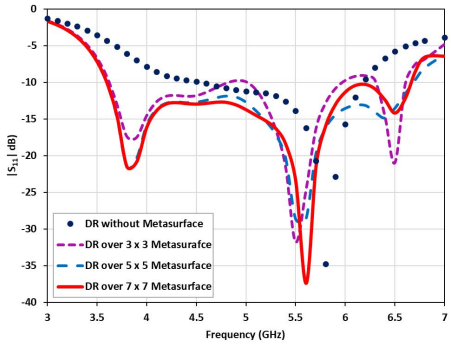

FIGURE 4. $|S_{11}|$ characteristics of antenna with and without metasurface.

Considering the above, the surface wave resonance property of the metasurface structure is exploited here for the design of the proposed CP DRA. To serve the purpose, a hybrid technique for the DRA using diagonal probe feed along with a well-matched metasurface is investigated and presented in this article. This method is demonstrated to achieve a wideband CP performance. By utilization of a plus-shaped unit cells-based metasurface extra resonances both in $|S_{11}|$ and AR can be generated, which is then fine-tuned by perturbing the upper probe (UP) of the coaxial feed, as demonstrated in Fig. 3 (a). Fig. 3 (b) shows that a very good impedance matching of 29.4% (3.6 GHz - 6.6 GHz) is achieved by optimizing UP to 1.1mm. Furthermore, it also improved the antenna's AR performance.

Fig. 4 depicts the $|S_{11}|$ characteristics of standalone DRA and DRA with 3 × 3, 5 × 5, and 7 × 7 metasurface, respectively. This comparison shows that DRA with 7 × 7 metasurface achieves multiple resonance responses with significant input matching. The reflection characteristics and AR performance of the optimized DRA before and after the metasurface is compared in Fig. 5 (a), 5 (b), and 5 (c), for $|S_{11}|$, VSWR, AR, and realized gain, respectively. The predicted 2:1-VSWR bandwidth of the antenna is shown in Fig. 5 (a), depicting higher VSWR bandwidth of DRA with metasurface as compared to DRA without metasurface. For DRA without metasurface, a single resonance occurs around 4.82 GHz with AR = 4.7 dB, indicating that the DRA without metasurface is not a CP (AR more than 5 dB) as shown in Fig. 5 (b). However, the DRA with metasurface achieves CP radiation depending upon the number of unit cells (N). Fig. 5 (b) also demonstrates the impact on the predicted AR range for a different number of unit cells (N). For $N = 3$ and $N = 5$, the multi-resonance response is observed which shifts first resonance towards the lower frequency range at 4.35 GHz (with AR = 0.8 dB and AR = 1.23 dB), while second resonance towards the higher frequency at 5.2GHz (with AR = 6.4 dB and AR = 0.66 dB), respectively. It is noteworthy that $N = 5$ also yields a third frequency resonance in the higher frequency range at 5.8 GHz (with AR = 2.4 dB), however, the overall trend does not satisfy the minimum AR requirement of <3-dB between 4.5 GHz and 5.1 GHz, resulting in a narrow 3-dB AR bandwidth. Finally, the optimized performance and desired CP performance are achieved by incrementing $N = 7$ with the two lowest AR values at 0.45 dB and 0.5 dB, discretely. It is also shown to achieve a wide 3-dB AR bandwidth of 19% ranging from 4.45 GHz to 5.39 GHz within the desired frequency range (2-VSWR).

The addition of metasurface on the ground extends the effective aperture of the antenna which leads to gain enhancement. Fig. 5 (c) provides a comparison of the realized gain. After placing DRA over the 7 × 7 metasurface, a gain improvement of 2.5 dB can be observed at the lower frequency band. Moreover, the DRA with metasurface shows a flat gain of 6 - 6.5 dBic across the frequency range from 3.8 GHz to 5.05 GHz, with a maximum gain value reaching up to 7.2 dBic at 4.75 GHz. Although a comparable performance is achieved in terms of $|S_{11}|$ and gain, the AR response of 7 × 7 metasurface stands out to be the best among these. Thus 7 × 7 metasurface is preferred over 3 × 3 and 5 × 5 metasurface.

To further understand the CP wave's generation phenomenon, the distributions of the electric fields are investigated and presented with cone visualizations. These time-dependent field distributions on the DRA, at 5.0 GHz for $\omega t = 0°$, 45°, 90°, and 180°, respectively are presented in Fig. 6. The circularly rotated behavior of these fields as observed from the DR with metasurface clearly recommends that the proposed DRA over metasurface undergoes a wideband CP radiation. Thus, it satisfies the requirement of the equal amplitude excitation of two orthogonal modes and a phase shift of 90° across a wide frequency range.

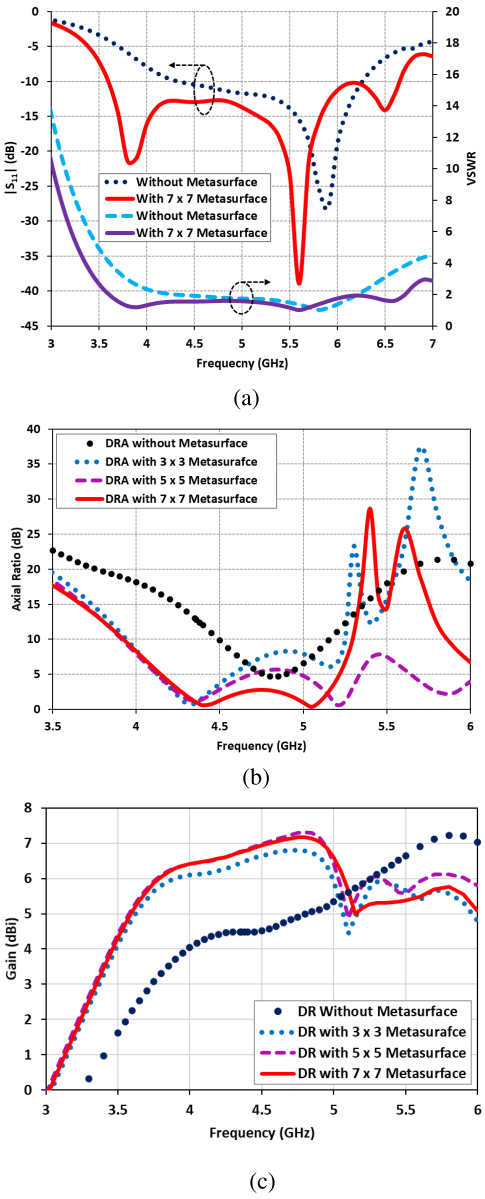

FIGURE 5. Antenna characteristics with and without metasurface (a) $|S_{11}|$ & VSWR (b) axial ratio (c) realized gain.

Furthermore, the clockwise rotation of electric fields is visible from Fig. 6, which confirms that the proposed antenna holds the characteristics of a left-hand circularly polarized (LHCP) radiation.

III. FABRICATION OF THE PROPOSED ANTENNA

A. PROTOTYPE AND MEASUREMENTS

For practical realization, the proposed DR antenna prototype was fabricated and is shown in Fig. 7 (a), 7 (b) and 7 (c), respectively. The metasurface is printed on top of a grounded FR4 substrate availing a standard etching technique. On the other hand, the rectangular DR is cut out of a TMM10i dielectric slab using the precision cutting facility. The prototype antenna is fed with a standard 50-Ω probe feed connector.

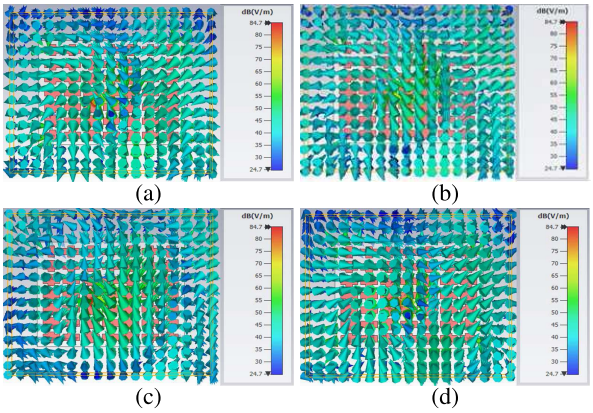

FIGURE 6. Clockwise rotating field distributions on the proposed DRA at 5.0 GHz for (a) $\omega t = 0°$ (b) 45° (c) 90° (d) 180°.

The required diameter of the upper probe UP of the feed is achieved by bonding a copper tape, referring to Fig. 7 (a).

Careful consideration is carried out to measure the probe thickness with Vernier caliper, before placing the DR on top of the metasurface, to minimize the fabrication losses. Once placed, the DR is fixed with the help of a thin adhesive tape, which has an insignificant impact on the radiation performance of the antenna. A fabricated prototype was then tested with PNA Vector Network Analyzer and an anechoic chamber to compute the antenna's impedance characteristics and its radiation performance, as demonstrated in Fig. 8 (a) and 8 (b).

B. $|S_{11}|$ CHARACTERISTICS

The predicted and measured $|S_{11}|$ results of the prototyped antenna is depicted in Fig. 9. These results are measured using an Agilent N5242A Vector Network Analyzer and are shown to be in good agreement with the predicted results. However, a slight shift can be observed from the $|S_{11}|$ plot. The second resonance takes its minimum value at 6 GHz against the predicted 5.5 GHz, which can be primarily ascribed to the fabrication tolerances (either bonded copper tape thickness or the hole drilled in the DR for probe feed). Due to smaller changes in physical length, the effective/radiating length changes are more significant on higher frequencies. It could be due to inconsistency of the bit used for the drilling of the feed hole, thus impacting the feed diameter, which leads to the difference. The measured $|S_{11}|$ offers a wide impedance bandwidth of 32% ranging from 3.6 GHz to 7 GHz. Similarly, the measured 2:1-VSWR bandwidth ranges 34% from 3.4 GHz to 7 GHz, complementing a wide impedance matching within the operational frequency range.

C. AR, GAIN AND RADIATION PATTERNS

The AR, gain, and radiation patterns of the fabricated metasurface-based DR antenna were measured by using the NSI-700S-50 spherical near-field chamber, available at the Australian Antenna Measurement Facility (AusAMF). These parameters are presented in Fig. 10, and Fig. 11, separately. Fig. 10 shows the antenna's predicted and measured AR.

TABLE 1. Comparison of the proposed wideband CP DRA with previously published literature based on wideband antennas.

Refs.	Antenna Structure	Impedance Bandwidth (%)	3-dB AR Bandwidth (%)	Gain (dBic)	Antenna Size ($\lambda_\circ \times \lambda_\circ \times \lambda_\circ$)
44	Metasurface over DR	17.2	NA	6.6	0.32 × 0.32 × 0.044 at 1.2 GHz
38	Patch + metasurface, capacitive loading	21.0	8.5	6.57	0.58 × 0.58 × 0.043 at 3.5 GHz
42	Patch + metasurface	17.0	14.5	>7.0	0.93 × 0.93 × 0.024 at 1.2 GHz
37	AMC Metasurface	33.07	15.92	5.76	0.37 × 0.37 × 0.18 at 2.5 GHz
36	Slot + metasurface	39.25	17.77	6.8	0.65 × 0.65 × 0.06 at 5.5 GHz
40	Rectangular loop + metasurface	19.0	11.4	7.53~8.2	0.75 × 0.75 × 0.06 at 5.8 GHz
47	Rectangular DRA	31.7	20	3.1~4.5	0.5 × 0.52 × 0.15 at 3.5 GHz
39	Patch +metasurface	20.6	17.4	8.0	0.79 × 0.79 × 0.067 at 5.8 GHz
48	Rectangular DRA with L-shaped slots	36.2	17.59	3.5~4.5	0.45 × 0.45 × 0.22 at 3.39 GHz
41	Patch + metasurface	14.3	14.3	4.8	0.86 × 0.67 × 0.13 at 5.60 GHz
Proposed	**DRA + metasurface**	**32.0**	**20.04**	**6.5~7.2**	**0.93 × 1.29 × 0.16 at 5.12 GHz**

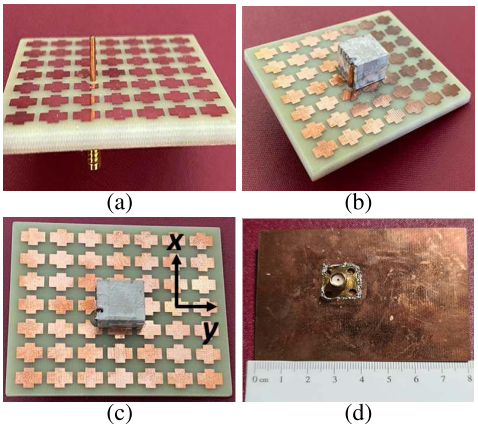

FIGURE 7. Fabricated prototype of the proposed antenna: (a) front view, (b) side view, and (c) top view (d) bottom view.

FIGURE 8. Measurement setup for computing measured results: (a) using VNA and (b) radiation characteristics using anechoic chamber setup.

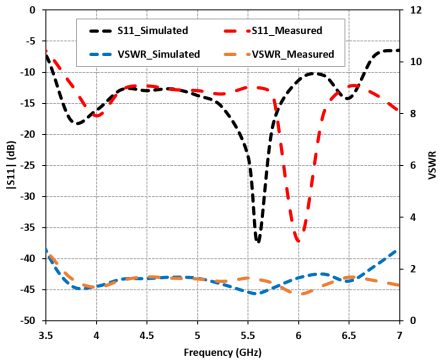

FIGURE 9. Comparison of predicted and measured antenna input matching including $|S_{11}|$ and VSWR.

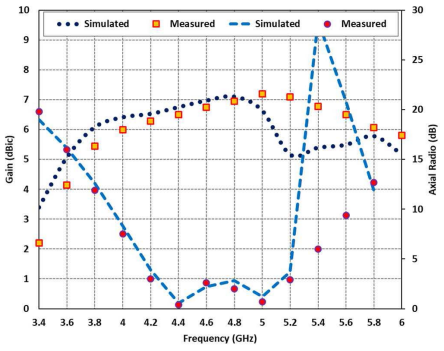

FIGURE 10. Comparison of predicted and measured antenna radiation characteristics including AR and gain.

The AR measurements are carried out by fixing the linearly polarized transmitting antenna and measuring the received signals of the CP DRA with 360° rotation method. Measured values for the AR are collected across all frequencies to get a frequency versus AR plot. A wide 3-dB AR bandwidth of 20.4% ranging from 4.2 GHz to 5.2 GHz is achieved, with a 0.5 dB increment and a slightly shifted response as compared to the predicted 19% 3-dB AR bandwidth ranging from 4.45 GHz to 5.39 GHz. This shift is similar to the measured $|S_{11}|$ plot and it can be attributed either by the fabrication/material tolerances or measurement errors due to the antenna's alignment and rotation in the anechoic chamber.

Fig. 10 also provides a comparison of the predicted and measured CP gain at the boresight. It can be observed that measured gain varies between 6-7 dBic across the operating frequency band. The measured gain values remain 0.5-1 dB below the predicted gain values at the lower frequency in the range of 3.4 GHz to 4.8 GHz. On the other hand, the gain values are 0.5-1 dB above the predicted gain values at the higher frequency range from 5.4 GHz to 6.0 GHz (off CP band) except for 1.8 dB at 5.2 GHz. The slight discrepancy in the gain values can be attributed to the antenna alignment in the anechoic chamber, as an experimental error.

D. FAR-FIELD RADIATION PATTERNS

The antenna's 3-D radiation patterns are presented in Fig. 11 at three different frequencies of 4.8 GHz, 5.0 GHz, and 5.4 GHz. The normalized predicted and measured radiation patterns are taken in two principal planes. LHCP radiation patterns are compared at these frequencies as plotted in Fig. 12, respectively. The antenna depicts quite stable

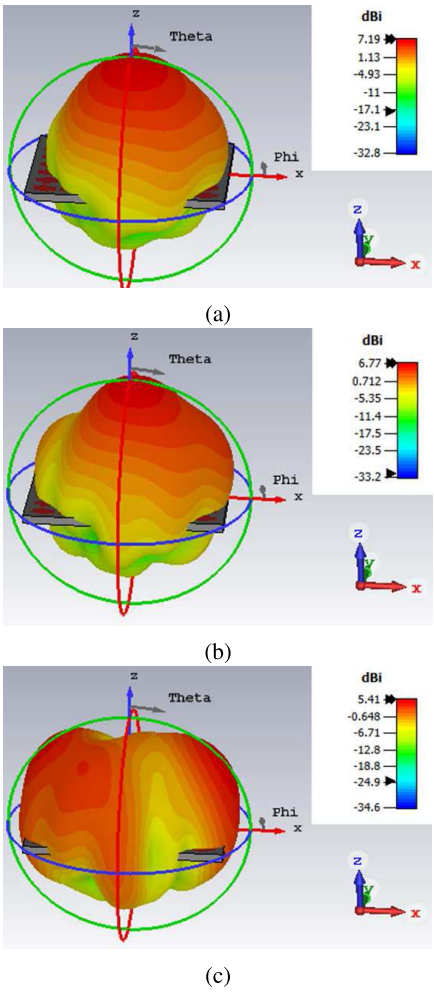

FIGURE 11. 3-D radiation patterns of antenna including the gain bar at (a) 4.8 GHz, (b) 5.0 GHz, and (c) 5.4 GHz.

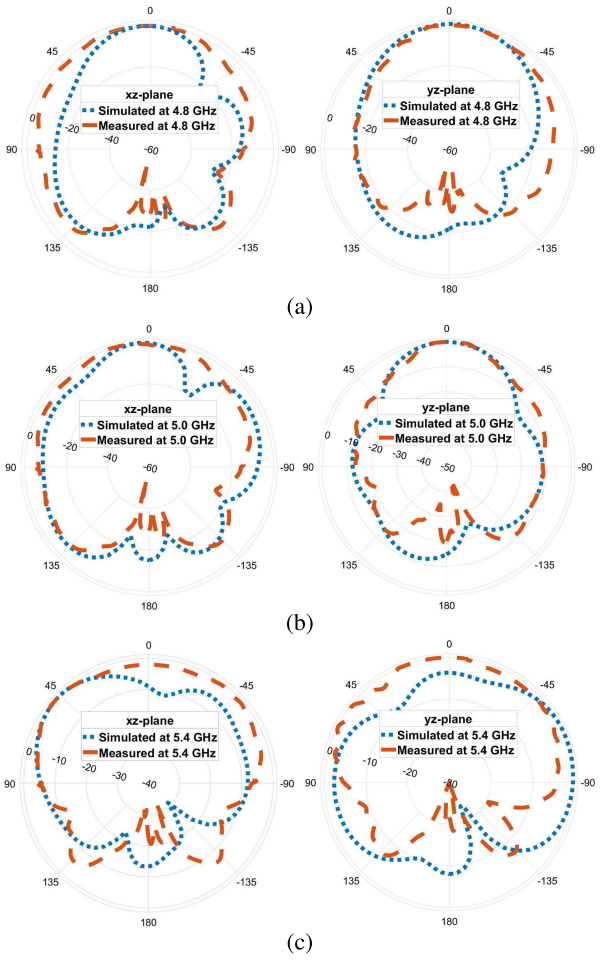

FIGURE 12. Predicted and measured radiation patterns (left-hand polarization) of antenna in two principal planes compared at (a) 4.8 GHz, (b) 5.0 GHz, and (c) 5.4 GHz.

radiation patterns in the broadside direction; however, a slight beam squinting has occurred at higher frequencies. Overall, the predicted and measured results show good agreement among them.

E. PERFORMANCE COMPARISON WITH EXISTING CP WIDEBAND ANTENNAS

This next section compares the proposed antenna's key performance parameters against the newly reported wideband CP hybrid antennas. For this purpose, a fair comparison is presented in Table 1 by selecting the recently published designs of wideband CP antennas integrating metasurfaces [35], [36], [37], [38], [39], [40], [41] and those of wideband DRA CP antennas [48], [49]. These antennas are compared in terms of their structure, 3-dB AR bandwidth, impedance bandwidth, gain, and antenna dimensions. From Table 1, the proposed antenna exhibits better AR bandwidth than those reported in [35], [36], [37], [38], [39], [40], [41], and [48], and [49], respectively. Furthermore, it is noteworthy that only the proposed antenna offers a rectangular DR over a metasurface, thus making it novel among this class of antennas.

IV. CONCLUSION

A low-profile, lightweight and single-fed wideband CP DR antenna over a metasurface has been presented and demonstrated experimentally. It uses a novel hybrid technique to realize wideband CP radiation characteristics. The technique is investigated to exploit the multi-resonance characteristics of a plus-shaped unit cell-based metasurface, with a strategic fed rectangular DR placed over it for performance improvement. The antenna radiation with the introduction of the metasurface is demonstrated to realize a wide bandwidth performance. The fabricated antenna with a compact size of $0.93\lambda_\circ \times 1.3\lambda_\circ \times 0.16\lambda_\circ$ exhibits a measured wide impedance bandwidth of 32% (3.6 GHz - 7 GHz) and an overlapping 3-dB AR bandwidth of 20.04% (4.2 GHz - 5.2 GHz), respectively. The novel yet simple design tends to reduce the complexity of staked layers, and it can be easily extendable for multi-band and high-gain CP array configurations.

REFERENCES

[1] A. C. Balanis, *Antenna Theory: Analysis and Design*, 2nd ed. New York, NY, USA: Wiley, 1997.
[2] S. Gao, Q. Lup, and F. Zhu, *Circularly Polarized Antennas*, 1st ed. New York, NY, USA: Wiley, 2014.

[3] Nasimuddin, Z. N. Chen, and X. Qing, "Dual-band circularly polarized S-shaped slotted patch antenna with a small frequency-ratio," *IEEE Trans. Antennas Propag.*, vol. 58, no. 6, pp. 2112–2115, Jun. 2010.

[4] Nasimuddin, K. P. Esselle, and A. K. Verma, "Wideband circularly polarized stacked microstrip antennas," *IEEE Antennas Wireless Propag. Lett.*, vol. 6, pp. 21–24, 2007.

[5] S. Drabowitch and A. P. Smith, *Modern Antennas*. New York, NY, USA: Springer, 2005.

[6] D. M. Pozar, *Microwave and RF Wireless Systems*. Hoboken, NJ, USA: Wiley, 2000.

[7] A. Petosa, *Dielectric Resonator Antenna Handbook*. Norwood, MA, USA: Artech House, 2007.

[8] K. P. Esselle, "A low-profile rectangular dielectric-resonator antenna," *IEEE Trans. Antennas Propag.*, vol. 44, no. 9, pp. 1296–1297, Sep. 1996.

[9] S. Trinh-Van, Y. Yang, K.-Y. Lee, and K. C. Hwang, "Single-fed circularly polarized dielectric resonator antenna with an enhanced axial ratio bandwidth and enhanced gain," *IEEE Access*, vol. 8, pp. 41045–41052, 2020.

[10] J. Iqbal, U. Illahi, M. I. Sulaiman, M. M. Alam, M. M. Su'ud, M. N. M. Yasin, and M. H. Jamaluddin, "Bandwidth enhancement and generation of CP by using parasitic patch on rectangular DRA for wireless applications," *IEEE Access*, vol. 7, pp. 94365–94372, 2019.

[11] K. W. Leung, W. C. Wong, K. M. Luk, and E. K. N. Yung, "Circular polarised dielectric resonator antenna excited by dual conformal strips," *Electron. Lett.*, vol. 36, no. 6, pp. 484–486, Mar. 2000.

[12] Y. Ge, K. P. Esselle, and T. S. Bird, "Compact dielectric resonator antennas with ultrawide 60%–110% bandwidth," *IEEE Trans. Antennas Propag.*, vol. 59, no. 9, pp. 3445–3448, Sep. 2011.

[13] K.-W. Khoo, Y.-X. Guo, and L. C. Ong, "Wideband circularly polarized dielectric resonator antenna," *IEEE Trans. Antennas Propag.*, vol. 55, no. 7, pp. 1929–1932, Jul. 2007.

[14] Y.-X. Sun, K. W. Leung, and J.-F. Mao, "Dualfunction dielectric resonator as antenna and phase-delay-line load: Designs of compact circularly polarized/differential antennas," *IEEE Trans. Antennas Propag.*, vol. 66, no. 1, pp. 414–419, Jan. 2018.

[15] S. A. A. Malekabadi, M. H. Neshati, and J. Rashed-Mohassel, "Circular polarized dielectric resonator antennas using a single probe feed," *Prog. Electromagn. Res. C*, vol. 3, pp. 81–94, 2008.

[16] M. T. K. Tam and R. D. Murch, "Circularly polarized circular sector dielectric resonator antenna," *IEEE Trans. Antennas Propag.*, vol. 48, no. 1, pp. 126–128, Jan. 2000.

[17] P. Patel, B. Mukherjee, and J. Mukherjee, "Wideband circularly polarized rectangular dielectric resonator antennas using square-shaped slots," *IEEE Antennas Wireless Propag. Lett.*, vol. 15, pp. 1309–1312, 2016.

[18] V. Hamsakutty, A. V. P. Kumar, J. Yohannan, and K. T. Mathew, "Coxial fed hexagonal dielectric resonator antenna for circular polarization," *Microw. Opt. Tech. Lett.*, vol. 48, no. 3, pp. 581–582, 2006.

[19] Y. M. Pan and K. W. Leung, "Wideband omnidirectional circularly polarized dielectric resonator antenna with parasitic strips," *IEEE Trans. Antennas Propag.*, vol. 60, no. 6, pp. 2992–2997, Jun. 2012.

[20] X. S. Fang and K. W. Leung, "Linear-/circular-polarization designs of dual-/wide-band cylindrical dielectric resonator antennas," *IEEE Trans. Antennas Propag.*, vol. 60, no. 6, pp. 2662–2671, Jun. 2012.

[21] Y. M. Pan and K. W. Leung, "Wideband circularly polarized trapezoidal dielectric resonator antenna," *IEEE Antennas Wireless Propag. Lett.*, vol. 9, pp. 588–591, 2010.

[22] H. Nawaz and A. Kiyani, "Ku-band dielectric resonator antenna array for microwave imaging," *Microw. Opt. Technol. Lett.*, vol. 58, no. 7, pp. 1651–1655, Jul. 2016.

[23] B. Rana and S. K. Parui, "Microstrip line fed wideband circularly-polarized dielectric resonator antenna array for microwave image sensing," *IEEE Sensors Lett.*, vol. 1, no. 3, pp. 1–7, Apr. 2017.

[24] S.-L.-S. Yang, R. Chair, A. A. Kishk, K.-F. Lee, and K.-M. Luk, "Study on sequential feeding networks for subarrays of circularly polarized elliptical dielectric resonator antenna," *IEEE Trans. Antennas Propag.*, vol. 55, no. 2, pp. 321–333, Feb. 2007.

[25] W.-W. Liu, Z.-H. Cao, and Z. Wang, "A wideband circularly polarized dielectric resonator antenna array," *IEEE Access*, vol. 9, pp. 99589–99594, 2021.

[26] M. Faenzi, G. Minatti, D. González-Ovejero, F. Caminita, E. Martini, C. D. Giovampaola, and S. Maci, "Metasurface antennas: New models, applications and realizations," *Sci. Rep.*, vol. 9, no. 1, pp. 1–14, Dec. 2019.

[27] S. S. Bukhari, J. Vardaxoglou, and W. Whittow, "A metasurfaces review: Definitions and applications," *Appl. Sci.*, vol. 9, no. 13, p. 2727, Jul. 2019.

[28] I. Park, "Application of metasurfaces in the design of performance-enhanced low-profile antennas," *EPJ Appl. Metamaterials*, vol. 5, p. 11, Dec. 2018.

[29] K. Agarwal, Nasimuddin, and A. Alphones, "RIS-based compact circularly polarized microstrip antennas," *IEEE Trans. Antennas Propag.*, vol. 61, no. 2, pp. 547–554, Feb. 2013.

[30] L. Bernard, G. Chertier, and R. Sauleau, "Wideband circularly polarized patch antennas on reactive impedance substrates," *IEEE Antennas Wireless Propag. Lett.*, vol. 10, pp. 1015–1018, 2011.

[31] F. Yang and Y. Rahmat-Samii, "A low profile single dipole antenna radiating circularly polarized waves," *IEEE Trans. Antennas Propag.*, vol. 53, no. 9, pp. 3083–3086, Sep. 2005.

[32] N. Nasimuddin, Z. N. Chen, and X. Qing, "Bandwidth enhancement of a single-feed circularly polarized antenna using a metasurface: Metamaterial-based wideband CP rectangular microstrip antenna," *IEEE Antennas Propag. Mag.*, vol. 58, no. 2, pp. 39–46, Apr. 2016.

[33] J. A. Sheersha, N. Nasimuddin, and A. Alphones, "A high gain wideband circularly polarized antenna with asymmetric metasurface," *Int. J. RF Microw. Comput.-Aided Eng.*, vol. 29, no. 7, Jul. 2019, Art. no. e21740.

[34] N. Hussain, M.-J. Jeong, A. Abbas, and N. Kim, "Metasurface-based single-layer wideband circularly polarized MIMO antenna for 5G millimeter-wave systems," *IEEE Access*, vol. 8, pp. 130293–130304, 2020.

[35] J. Dong, C. Ding, and J. Mo, "A low-profile wideband linear-to-circular polarization conversion slot antenna using metasurface," *Materials*, vol. 13, no. 5, p. 1164, Mar. 2020.

[36] M. Ameen and R. K. Chaudhary, "Metamaterial-based wideband circularly polarised antenna with rotated V-shaped metasurface for small satellite applications," *Electron. Lett.*, vol. 55, no. 7, pp. 365–366, Apr. 2019.

[37] Y. Juan, W. Yang, and W. Che, "Miniaturized low-profile circularly polarized metasurface antenna using capacitive loading," *IEEE Trans. Antennas Propag.*, vol. 67, no. 5, pp. 3527–3532, May 2019.

[38] L. Yuan, H. Yu-Xuan, L. Zhan-Wei, C. Shu-Ting, X. Xiao-Ming, and G. Jing, "Design of a compact wideband CP metasurface antenna," *Int. J. RF Microw. Comput.-Aided Eng.*, vol. 30, no. 10, Oct. 2020, Art. no. e22332.

[39] Y. Liu, Y.-X. Huang, Z.-W. Liu, S.-T. Cai, X.-M. Xiong, and J. Guo, "A new broadband circularly polarized antenna with a single-layer metasurface," *Int. J. RF Microw. Comput.-Aided Eng.*, vol. 30, Jul. 2020, Art. no. e22226.

[40] N. Hussain, I. S. Naqvi, A. W. Awan, and T. T. Le, "A metasurface-based wideband bidirectional same-sense circularly polarized antenna," *Int. J. RF Microw. Comput.-Aided Eng.*, vol. 30, Aug. 2019, Art. no. e22262.

[41] S. Liu, D. Yang, and J. Pan, "A low-profile circularly polarized metasurface antenna with wide axial-ratio beamwidth," *IEEE Antennas Wireless Propag. Lett.*, vol. 18, no. 7, pp. 1438–1442, Jul. 2019.

[42] Y. Qiu, Z. Weng, J. Liu, and B. He, "DRA-fed broadband metasurface antennas using characteristic mode analysis," in *Proc. Int. Symp. Antennas Propag. (ISAP)*, Xi'an, China, Oct. 2019, pp. 1–3.

[43] S.-K. Zhao, N.-W. Liu, Q. Chen, G. Fu, and X.-P. Chen, "A low-profile dielectric resonator antenna with compact-size and wide bandwidth by using metasurface," *IEEE Access*, vol. 9, pp. 29819–29826, 2021.

[44] *CST Microwave Studio, Version 2016.04*, SIMULIA, Dassault Syst., France, Jul. 2016.

[45] A. Kiyani, Nasimuddin, and K. P. Esselle, "A wideband circularly polarized dielectric resonator antenna over a metasurface," in *IEEE Int. Symp. Antennas Propag. USNC/URSI Nat. Radio Sci. Meeting*, Boston, MA, USA, Jul. 2018, pp. 2085–2086.

[46] F. Costa, O. Luukkonen, C. R. Simovski, A. Monorchio, S. A. Tretyakov, and P. M. de Maagt, "TE surface wave resonances on high-impedance surface based antennas: Analysis and modeling," *IEEE Trans. Antennas Propag.*, vol. 59, no. 10, pp. 3588–3596, Oct. 2011.

[47] D. Sievenpiper, L. Zhang, R. F. J. Broas, N. G. Alexopolous, and E. Yablonovitch, "High-impedance electromagnetic surfaces with a forbidden frequency band," *IEEE Trans. Microw. Theory Techn.*, vol. 47, no. 11, pp. 2059–2074, Nov. 1999.

[48] R. Kumari and R. K. Gangwar, "Circularly polarized rectangular dielectric resonator antenna fed by a cross aperture coupled spiral microstrip line," *Int. J. RF Microw. Comput.-Aided Eng.*, vol. 28, no. 2, Feb. 2018, Art. no. e21200.

[49] R. Kumar, S. R. Thummaluru, and R. K. Chaudhary, "Improvements in Wi-MAX reception: A new dual-mode wideband circularly polarized dielectric resonator antenna," *IEEE Antennas Propag. Mag.*, vol. 61, no. 1, pp. 41–49, Feb. 2019.

ARSLAN KIYANI (Member, IEEE) received the B.Sc. degree in electrical (telecommunications) engineering from the COMSATS Institute of Information Technology (CIIT), Islamabad, Pakistan, in 2011, the M.S. degree in electrical engineering from Universiti Tun Hussein Onn Malaysia (UTHM), Johor, Malaysia, in 2014, and the M.Res. and Ph.D. degrees in electronics engineering from Macquarie University, Sydney, Australia, in 2016 and 2021, respectively. His research interests include reflectarrays, sparse arrays, Fabry-Perot cavity antennas, planar metasurface-based antennas, and dielectric resonator antennas. He was a recipient of the 2022 International Union of Radio Science (URSI) Young Scientist Award and the 2020 IEEE NSW Section Outstanding Young Professional of the Year Award. He has also received several research grants and scholarships, including the Prototype Research Grant Scheme (PRGS), Graduate Research Incentive Grant (GIPS), and Fundamental Research Grant Scheme (FRGS) for the M.S. degree, International Research Training Program Scholarship (iRTP) for the M.Res. degree, and Macquarie University Research Excellence Scholarship (MQRES) for the Ph.D. degree. More recently, he has been awarded the Macquarie University COVID Recover Fellowship. He is also an Olympiad Winner of the antenna design competition at the Ghulam Ishaq Khan University (GIKI), Pakistan, and also a recipient of a Semi-Grand Prize (Gold Medal and Special Trophy) and two gold medals for his research products exhibited at various international invention and research exhibitions in Malaysia and South Korea, respectively.

NASIMUDDIN NASIMUDDIN (Senior Member, IEEE) received the B.Sc. degree in New Delhi, India, in 1994, and the M.Tech. degree in microwave electronics and the Ph.D. degree from the University of Delhi, India, in 1998 and 2004, respectively.

From 1999 to 2003, he has worked as a Senior Research Fellow with the DST sponsored project on Optical Control of Passive Microwave Devices and Council of Scientific and Industrial Research (CSIR), Government of India, awarded a Senior Research Fellowship in engineering science for the project titled Investigations of Microstrip Antennas as a Sensor for Determination of Complex Dielectric Constant of Materials at the Department of Electronic Science, University of Delhi. From 2004 to 2006, he was worked as an Australian Postdoctoral Research Fellow in awarded Discovery project grant from the Australian Research Council for the project titled Microwave Sensor Based on Multilayered Microstrip Patch/Line Resonators at Macquarie University, Australia. He is currently a Scientist with the Institute for Infocomm Research, A*STAR, Singapore. He has published 185 journals and conference technical papers on microstrip-based microwave antennas and components. He has edited and contributed a chapter to a book *Microstrip Antennas* (InTech, 2011). He has been filed five antenna patent applications and several antenna technologies licenses to companies. His research interests include multilayered microstrip-based structures, millimeter-wave antennas, radiofrequency identification reader antennas, global positioning systems/global navigation satellite systems, ultrawideband antennas, metamaterials-based microstrip antennas, beamforming/beam-steering antennas, satellite antennas, RF energy harvesting systems, circularly polarized microstrip antennas, and small antennas for TV white space communications. He is a Senior Member of the IEEE Antennas and Propagation Society and an Executive Committee Member of the IEEE MTT/AP Chapter/CRFID Chapter Singapore. He has also been an organizing committee member of international/national conferences related to antenna and propagation. He was awarded a Senior Research Fellowship from the Council of Scientific and Industrial Research, Government of India in Engineering Science, from 2001 to 2003, a Discovery Projects Fellowship from the Australian Research Council, from 2004 to 2006, the Singapore Manufacturing Federation Award (with project team), in 2014, and the Young Scientist Award from the International Union of Radio Science (URSI), in 2005.

RAHEEL M. HASHMI, photograph and biography not available at the time of publication.

AFFAN AZIZ BABA (Member, IEEE) received the B.S. degree (Hons.) in electrical (telecommunication) engineering from the COMSATS Institute of Information Technology (CIIT), Islamabad, Pakistan, in 2011, the M.S. degree in electrical and electronics engineering from Universiti Teknologi PETRONAS, Malaysia, in 2014, and the Ph.D. degree in electronics engineering from Macquarie University, Australia, in 2018. His current research interests include mm-wave wideband passive beam steering antennas, highly efficient on-chip antennas, wideband Fabry-Perot cavity antennas, electromagnetic bandgap structures, frequency selective surfaces, millimeter-wave antennas, and dielectric resonator antennas. He received the IMQRES, in 2014, and the International Postgraduate Scholarship from Universiti Teknologi Petronas, in 2011.

SYED MUZAHIR ABBAS (Senior Member, IEEE) received the B.Sc. degree in electrical (telecommunication) engineering from the COMSATS Institute of Information Technology (CIIT), Islamabad, Pakistan, in 2006, the M.Sc. degree in computer engineering from the Center for Advanced Studies in Engineering (CASE), Islamabad, in 2009, and the Ph.D. degree in electronics engineering at Macquarie University, North Ryde, NSW, Australia, in 2016. He has been a Transmission Engineer at Alcatel-Lucent, Pakistan, a RF Engineer with CommScope, Australia, and a Senior Antenna Design Engineer with Benelec Technologies, Australia. He has lectured various courses at CIIT, Western Sydney University, Australia, Macquarie University, and The University of Sydney, Australia. He is currently working as a Senior Principal Engineer with Benelec Technologies. He has been a Visiting Researcher with the ElectroScience Laboratory, The Ohio State University, USA, and Queen Mary University of London, U.K. His research interests include base station antennas, mmWave antennas, high-impedance surfaces, frequency selective surfaces, flexible/embroidered antennas, CNT yarns, CNT/graphene-based antennas, reconfigurable antennas/electronics, and the development of antennas for UWB and WBAN applications. He has also received several prestigious awards and fellowships, including the 2012 iMQRES Award for Ph.D. degree, the Research Productivity Awards from CIIT, in 2012 and 2010, the 2013 CSIRO Postgraduate Fellowship, the 2018 Young Scientist Award (Commission B—Field and Waves) from the International Union of Radio Science (URSI), the 2019 IEEE NSW Outstanding Young Professional Award, and the 2020 IEEE 5G World Forum Best Paper Award.

KARU P. ESSELLE (Fellow, IEEE) received the B.Sc. degree (Hons.) in electronic and telecommunication engineering from the University of Moratuwa, Sri Lanka, and the M.A.Sc. and Ph.D. degrees (Hons.) in electrical engineering from the University of Ottawa, Canada.

He is currently the Distinguished Professor in electromagnetic and antenna engineering with the University of Technology Sydney and a Visiting Professor with Macquarie University, Sydney. According to the 2019 special report on research published by The Australian national newspaper, he is the National Research Field Leader in Australia in both microelectronics and electromagnetism fields. Previously, he was the Director of the WiMed Research Centre and the Associate Dean of Higher Degree Research (HDR) of the Division of Information and Communication Sciences and directed the Centre for Collaboration in Electromagnetic and Antenna Engineering, Macquarie University. He has also served as a member of the Dean's Advisory Council and the Division Executive and the Head of the Department several times. He has authored over 650 research publications and his papers have been cited 12,500 times. In 2021, his publications received over 1,400 citations. His H-index is 53 and i-10 is 212. Often one or two of his papers are ranked by Web of Science and Clarivate as Highly Cited Papers (top 1% in the academic field of Engineering). For example, two papers are ranked so, for citations received, in January 2022 and February 2022. Some papers have been ranked as Hot Papers as well (top 0.1% in Engineering), e.g., A Scientific Reports paper for citations received, in January 2022 and February 2022. Since 2002, his research team has been involved with research grants, contracts, and Ph.D. scholarships worth over 22 million dollars, including 15 Australian Research Council grants, without counting the 245 million-dollar SmartSat Corporative Research Centre, which started, in 2019. His research has been supported by many national and international organizations, including Australian Research Council, Intel, U.S. Air Force, Cisco Systems, Hewlett-Packard, Australian Department of Defence, Australian Department of Industry, NSW Chief Scientist and Engineer Office, and German and Indian governments.

Dr. Karu is a fellow of the Royal Society of New South Wales and Engineers Australia, and the Director of Innovations for Humanity Pty Ltd. His most recent awards include the top Space award in Australia—the ''Winner of Winners'' Excellence Award and the Academic of Year Award at the 2022 Australian Space Awards, Engineers Australia 2022 Sydney Professional Engineer of the Year, both the most prestigious Excellence Award and the Academic of the Year Award at 2021 Australian Defence Industry Awards. He was one of the Finalist of 2021 Australian National Eureka Prize for Outstanding Mentor of Young Researchers and Runner-up to the same prize, in 2020. He received the 2019 Motohisa Kanda Award (from IEEE USA) for the most cited paper in IEEE TRANSACTIONS ON ELECTROMAGNETIC COMPATIBILITY in the past five years, the 2021 IEEE Region 10 (Asia-Pacific) Outstanding Volunteer Award, and the 2020 IEEE NSW Outstanding Volunteer Award. In addition to the IEEE Kanda Award mentioned above, several of his papers have been among most cited or most downloaded. He is currently shortlisted as one of the five finalists for the forthcoming Australian national 2022 Professional Engineers of the year title. Previously, he received the 2004 Innovation Award for best invention disclosure, the 2009 Vice Chancellor's Award for Excellence in Higher Degree Research Supervision, the 2012 and 2016 Engineering Excellence Awards for Best Published Paper from IESL NSW Chapter, the 2011 Outstanding Branch Counsellor Award from IEEE headquarters (USA), 2017 Excellence in Research Award from the Faculty of Science and Engineering, the 2017 Engineering Excellence Award for Best Innovation, the 2017 Highly Commended Research Excellence Award from Macquarie University, the 2017 Certificate of Recognition from IEEE Region 10, the 2019 Macquarie University Research Excellence Award for Innovative Technologies, and the 2019 ARC Discovery International Award. His mentees have been awarded many fellowships, awards, and prizes for their research achievements. 85 international experts who examined the theses his Ph.D. graduates ranked them in the top 5% or 10%. Two of his students were awarded Ph.D. degree (Hons.) at Macquarie University—the Vice Chancellor's Commendation, and one received University Medal for Master of Research. He has provided expert assistance to more than a dozen companies, including Intel, the Hewlett Packard Laboratory (USA), Cisco Systems (USA), Audacy (USA), Cochlear, Optus, ResMed, and Katherine-Werke (Germany). He led the team that designed the high-gain antenna system for the world's first entirely Ka-band CubeSat made by Audacy, USA, and launched to space by SpaceX, in December 2018. This is believed to be the first Australian-designed high-gain antenna system launched to space, since CSIRO-designed antennas in Australia's own FedSat launched, in 2002. He is in the College of Expert Reviewers of the European Science Foundation (2019–2022) and he has been invited to serve as an International Expert/a Research Grant Assessor by several other research funding bodies as well, including the European Research Council and funding agencies in Norway, Belgium, The Netherlands, Canada, Finland, Hong Kong, Georgia, South Africa, and Chile. He has been invited by vice-chancellors of Australian and overseas universities to assess applications for promotion to professorial levels. He has also been invited to assess grant applications submitted to Australia's most prestigious schemes, such as Australian Federation Fellowships and Australian Laureate Fellowships. In addition to the large number of invited conference speeches he has given, he has been an Invited Plenary Speaker/an Extended Speaker/a Keynote Speaker/a Distinguished Speaker of several IEEE and other venues over 30 times, including EuCAP 2020 Copenhagen, Denmark; URSI'19, Seville, Spain; and 23rd ICECOM 2019, Dubrovnik, Croatia. From 2018 to 2020, he chaired the prestigious Distinguished Lecturer Program Committee of the IEEE Antennas and Propagation (AP) Society—the premier global learned society dedicated for antennas and propagation, which has close to 10,000 members worldwide. After two stages in the selection process, he was also selected by this Society as one of two candidates in the ballot for the 2019 President of the Society. Only three people from Asia or Pacific apparently have received this honour in the 68-year history of this Society. He is also one of the three distinguished lecturers (DL) selected by the Society, in 2016. He is the only Australian to Chair the AP DL Program ever, the only Australian AP DL in almost two decades, and second Australian AP DL ever (after UTS Distinguished Visiting Professor Trevor Bird). He has served the IEEE AP Society Administrative Committee in several elected or ex-officio positions (2015–2020). He is also the Chair of the Board of Management of Australian Antenna Measurement Facility, and was the Elected Chair of IEEE New South Wales (NSW), and IEEE NSW AP/MTT Chapter, in 2016 and 2017. He is the Track Chair of IEEE AP-S/URSI 2022 Denver, Singapore, in 2021, and Montreal, in 2020, the Technical Program Committee Co-Chair of ISAP 2015, APMC 2011, and TENCON 2013, and the Publicity Chair of ICEAA/IEEE APWC 2016, IWAT 2014, and APMC 2000. He has served or is serving as a Senior Editor of IEEE ACCESS, an Associate Editor of IEEE TRANSACTIONS ON ANTENNAS PROPAGATION, *IEEE Antennas and Propagation Magazine*, and IEEE ACCESS, and the Lead Guest Editor of several journals, including IEEE ANTENNAS AND WIRELESS PROPAGATION LETTERS. His research activities are posted in the web at (http://web.science.mq.edu.au/~esselle/ and https://www.uts.edu.au/staff/karu.esselle).

ABDELHADY MAHMOUD (Member, IEEE) received the B.Sc. (Hons.) and M.Sc. degrees in electrical engineering from Benha University, Benha, Egypt, in 2000 and 2005, respectively, and the Ph.D. degree in electrical engineering from Menoufia University, Egypt, in 2013. From 2010 to 2012, he was a Ph.D. Researcher with the State Key Laboratory of MillimeterWave, Nanjing, China. From 2013 to 2015, he was a Postdoctoral Fellow with Concordia University, Montreal, QC, Canada. He is currently an Associate Professor with the Department of Electrical Engineering, Faculty of Engineering, Benha University. His current research interests include the design of RFID passive tags, artificial lens, circularly polarized, and linearly polarized reflectarrays and transmitarrays, MIMO, 3-D printed structure, broadband circularly polarized dielectric resonator antennas, and polarizer twisting structures at microwave and millimeter-wave frequencies.